PLEA 2020 A CORUÑA
Planning Post Carbon Cities

Automated Computer Vision Recognition Based Method to Determine Glare Causing Patches on Reflective Building Façades

RANIA LABIB[1], MARK CLAYTON[2]
[1]Prairie View A&M University, Prairie View, Texas, USA
[2]Texas A&M University, College Station, Texas, USA

1. INTRODUCTION

The abundant use of highly reflective cladding in dense urban areas is causing severe visual discomfort because of reflection of the sunlight that falls on those surfaces. These intense reflections can cause a disabling glare that impairs the vision of the occupants of surrounding buildings [1–3].

Glare impairs visual performance and well-being, leading to premature fatigue, headaches, blurred vision, and eyestrain. Glare problems can worsen in office environments in which there is a need for frequent and extended computer usage. The increasing use of various digital technologies in offices can create substantial challenges for office occupants in processing information and performing visual tasks throughout the day [4–9], and creating a visually comfortable environment in office areas could help reduce the strain on workers' eyes that must constantly adapt to different visual tasks and thus ultimately increase workers' productivity.

In addition to the glare problem, reflective building elements reflect sunlight onto surrounding vegetation, causing burn damage. An example of reflective building cladding causing glare and vegetation burn was experienced in Dallas, Texas, where the façade of a 42-story high-rise residential tower, which was fitted with a highly reflective glazing, caused intense specular reflections into the Nasher sculpture museum. This resulted in overheating of the interior spaces of the museum, leading to the damage and deterioration of the sculptures on display [10,11]. The sunlight was also reflected onto the Nasher museum's garden, creating hot spots in both exposed and shaded sections of the garden. Daily readings by museum officials recorded temperatures at those hot spots that were approximately 40 degrees higher than the air temperature [10].

Glare in buildings is usually assessed by analyzing the luminance values in 180-degree fisheye high dynamic range (HDR) images or renderings. The analysis outputs the daylight glare probability (DGP) value and highlights glare sources on reflective surfaces. However, the highlighted glare sources' actual locations on the reflective surface are difficult to determine using the analyzed images due to the skewed fisheye projection.

This research paper proposes a methodology that facilitates the determination of the exact location of glare-causing façade panels using OpenCV (Open Source Computer Vision Library), an open source computer vision and machine learning software library [12]. In addition to being an automated method, it can be applied to large-scale glare simulations that consist of hundreds or even thousands of glare images.

In this study, 15 views inside a small building that faced a tower fitted with a reflective façade were analyzed for glare over the course of an entire year. The HDR renderings produced were further examined using custom software written in Python, a programming language [13] that utilizes computer vision recognition.

2. GLARE ANALYSIS USING HDR RENDERINGS

180-degree fisheye HDR renderings have been used in assessing glares caused by a high ratio of luminance between the task that is being looked at and the glare source. HDR rendering can represent the full dynamic range from the brightest light (direct sunlight) to the darkest spots, such as deep shadow, in the examined scene, making it one of the best tools to assess glare [14–16]. Glare simulations and HDR renderings usually use CIE standard clear sky [17].

The HDR images are usually analyzed using Radiance, which is an open source software for accurate lighting simulation and visualization based on a backward ray-tracing algorithm [18].

3. METHODOLOGY

As noted, this paper proposes an computer vision recognition based method to accurately determine the patches on a specific reflective façade that cause glare during every hour of the year. Glare analysis was

35th PLEA Conference. Planning Post Carbon Cities.
DOI: https://doi.org/10.17979/spudc.9788497497947

performed from 15 views inside a small building located across from a 11-story tower. The geometric model of both buildings, the glare analysis process, and the computer vision recognition algorithm are explained in the next three sections.

3.1 THE GEOMETRIC MODEL

A geometric model of two buildings—a three-floor building and a tower—was created with the Rhinoceros 3D modeling software [19]. The location of the buildings was set to Houston, Texas, in the United States. The latitude of Houston is 29.76°N, the longitude is -95.36°W, and its elevation is 80 ft (24.4 m) above sea level.

The tower consists of 11 floors, and it is 108 ft (33 m) tall and 59 ft (18 m) wide. Each floor has seven rooms measuring 16 x 13 ft (5 x 4 m) with a ceiling height of 9.8 ft (3 m). The smaller building consists of three floors, and it is 29.5 ft (9 m) tall and 42.7 ft (13 m) wide. Each floor has five rooms measuring 16 x 13 ft (5 x 4 m) with a ceiling height of 9.8 ft (3 m). The street width between the buildings is 98.5 ft (30 m) (Figure 4). The reflective façade is oriented toward the south. Figure 1 shows the geometric model that includes context buildings on both sides of the tower to mimic an urban context.

In the modeled buildings, the façade of the tower is considered to be a glare-causing surface due to its high reflectance and its orientation toward the south.

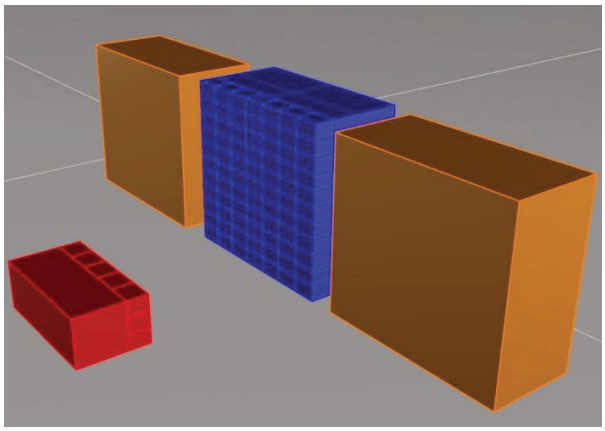

Figure 1. The modeled 11-story tower (blue), the three-floor building (red), and the context buildings (brown).

3.2 GLARE ANAYLSIS

A view inside each room in the small building was created at a height of 5'6" and located in the center of the room as one looks toward the reflective building façade. The total number of views was 15. In order to assess and quantify the glare caused by the reflective façade, each view was rendered to HDR 180-fisheye images, which were further analyzed to obtain the DGP value for each hour of the year (HoY). Several glare indices have been developed over the past decade to assess glare in views within interior spaces, but it was determined that DGP was the most suitable metric to use for this study. DGP was developed by Wienold and Christoffersen and based on laboratory studies in daylit spaces in two different locations (Freiburg, Germany, and Copenhagen, Denmark) in order to assess glare. That study tested 72 different objects under various daylighting conditions, and DGP showed a remarkably high correlation with users' glare perceptions [20].

In addition to calculating the DGP, the HDR renderings were used to visualize the glare sources in each scene. Glare sources in HDR renderings are usually highlighted in random colors by Radiance. Figure 2 shows an example of the HDR renderings produced of the 15 views, with the glare sources automatically highlighted in different colors by Radiance.

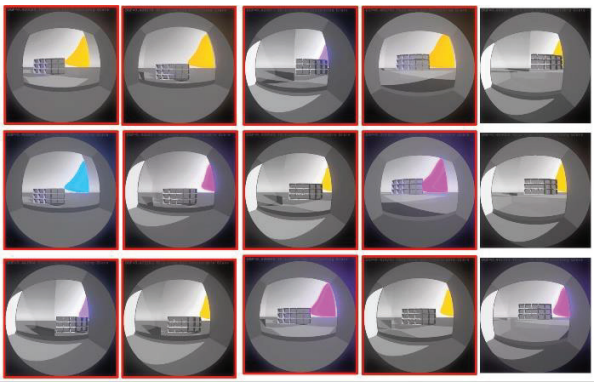

Figure 2. HDR 180-fisheye renderings of 15 views inside the three-story building looking outward. The HDR renderings are used for glare analysis. Glare sources are automatically highlighted by Radiance in random colors, such as magenta, yellow, or cyan.

3.3 High Performance Computing

The total number of HDR renderings needed to analyze glare in all 15 views for every HoY was 65,000. Each rendering took about 111 seconds to complete on a high-end desktop computer [21], meaning that running the glare simulations could take about 83 days. It is evident that carrying out such large-scale hourly glare simulations can be a complicated process due to the intensive computing power that is required. Furthermore, running such simulations manually is impossible because of the enormous number of files that are needed for the simulation process. To mitigate these challenges, the simulations were automated with Python, and executed on a high performance computing (HPC) environment using the parallel computing framework proposed by Labib and Baltazar [21]. HPC facilitated the execution of such large number of files on

35th PLEA Conference. Planning Post Carbon Cities.
DOI: https://doi.org/10.17979/spudc.9788497497947

powerful computing nodes that run in parallel to speed up the process of running such a large-scale simulation in just a few hours.

3.4 COMPUTER VISION RECCOGNITION

Because of the enormous number of HDR renderings produced following the glare analysis and considering their skewed projection, it is evident that locating the glare-causing façade panels manually would be impossible. It was therefore determined that an artificial intelligence-based method—specifically, computer vision recognition—would be necessary for this step, the workflow for which is shown in figure 3.

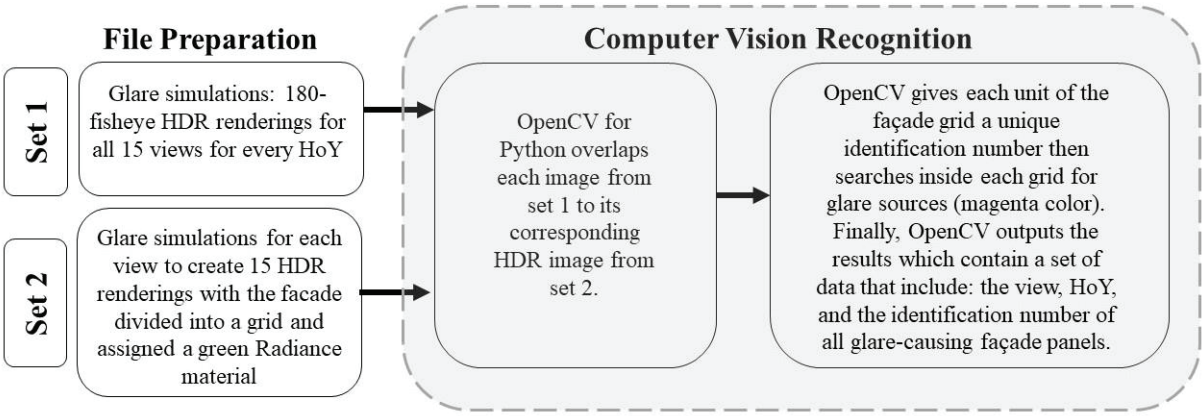

Figure 3. The workflow for locating the façade panels causing glare for every HoY using computer vision recognition.

The 180-degree fisheye images that resulted from the glare analysis were further examined by custom-written Python software that utilized advanced features of OpenCV. To facilitate locating the glare-causing façade panels by OpenCV, each view was rendered to produce images containing a green mask on the reflective façade. In addition to the mask, the façade was also divided into a 5 x 4m grid. To produce these images, each view (total 15 views) was rendered using custom Radiance materials that were assigned to the interior of the room, the outside ground, and the façade, which was given a Radiance plastic material with the RGB value of (0,255,0). To produce a grid system, black-colored mullions were modeled and rendered on top of the façade using a Radiance material with an RGB value of (0,0,0). The mullion system was used to divide the façade into patches that were 5m wide and 3m high; see figure 4.

The Python script overlaid each HDR rendering produced for every view for every HoY from the initial set of glare simulations onto the corresponding rendering that was prepared with a grid on top of the reflective façade, as shown in figure 5. The program looked for glare sources only in the green-masked grid (the reflective façade) and located the glare sources in each view inside the grid units. Each grid unit was assigned a unique identification number (ID) by the Python program. The software package that was used to write and send the files to Radiance originally included instructions to output the HDR images with randomly colored highlighting, as shown in figure 2. However, the Python script was designed to look for one specific color (magenta), so it was necessary for the commands sent to Radiance to be customized so that Radiance output the glare in magenta only, with an RGB value of (255, 0, 255).

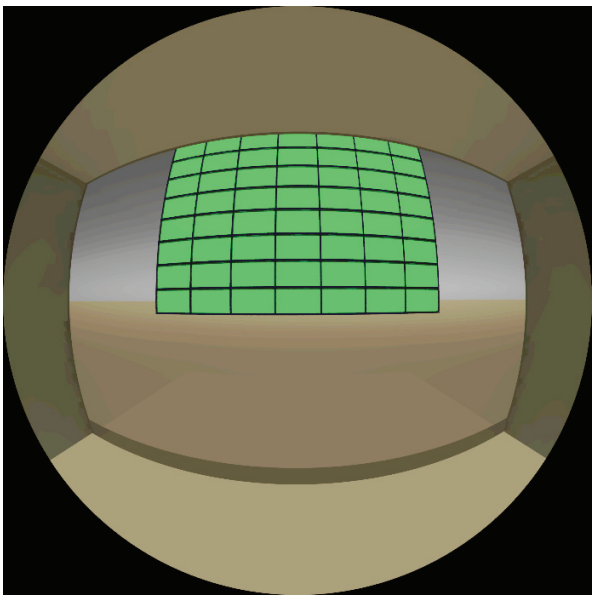

Figure 4. A custom HDR rendering of one view showing the reflective façade, which was assigned a green Radiance material, with a 5 x 3m mullion system modeled on top of it.

35th PLEA Conference. Planning Post Carbon Cities.
DOI: https://doi.org/10.17979/spudc.9788497497947

After the pictures were overlaid, Python's OpenCV tools facilitated locating the magenta color inside each grid.

Figure 5 shows a visualization of the output of the Python script. A grid with the letter P indicates that the façade panel represented by the grid causes glare at that HoY, and a grid with the letter N indicates that it does not.

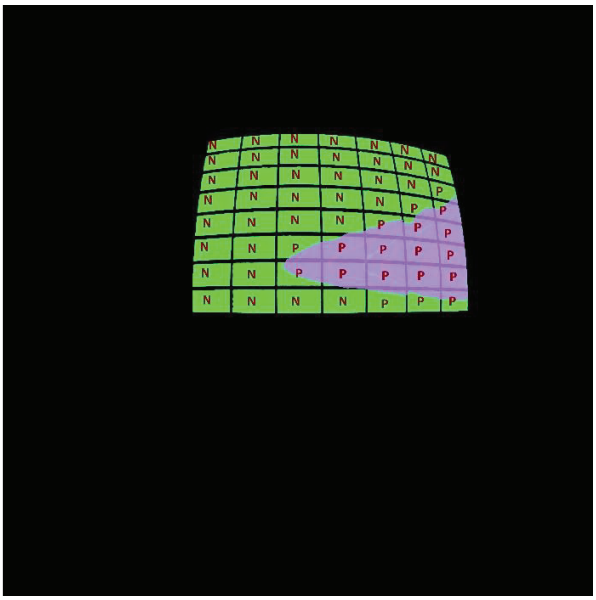

Figure 5. A visualization of the results of the Python/OpenCV code that facilitated the overlaying of an image from the glare simulations (set 1) with the corresponding mask (set 2). P in each grid unit indicates the presence of a glare source (magenta color) in that unit. N indicates no glare sources in the grid unit.

Finally, the results from the glare-causing panel program were output and the data stored in a SQL database for easy access. The data included the view, HoY, and ID of the grid unit; see figure 6.

4. RESULTS

Upon executing the Python/OpenCV program, a SQL database was created. The database contained the location of the glare sources in each of the 15 examined views for every HoY, for a total of 65,000 views. The locations of the glare sources were expressed by the façade grid ID.

5. CONCLUSION

The Python program facilitated the determination of the exact locations of the glare-causing panels on a reflective façade, a process that has never been possible before using traditional fisheye HDR images due to their skewed projection. The Python program also executes in an automated manner, thus eliminating manual processing efforts, making the proposed method time-efficient, especially for large-scale analyses that consist of thousands of images. Furthermore, the proposed computer vision process outputs the results of the glare analysis in an easy-to-read manner, making it an easy and quick process to search for and extract glare information about a specific view at a specific HoY. Because the obtained information locates the glare sources in occupants' views, it becomes a great asset, especially in the early design process when architects

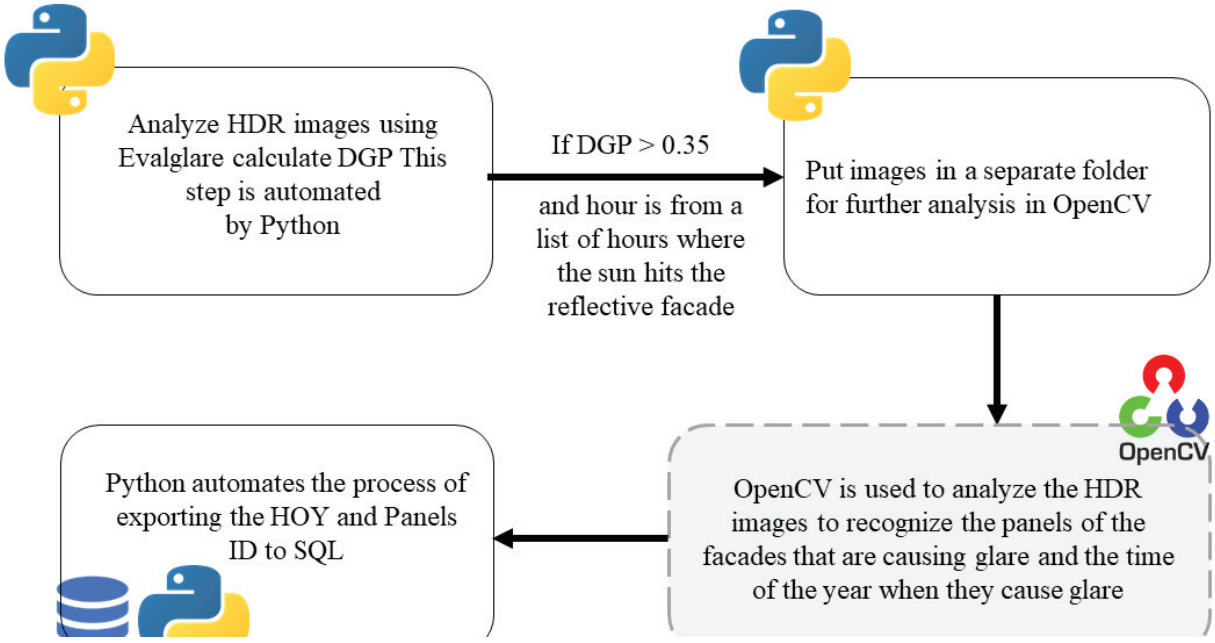

Figure 6. The overall workflow of the Python and OpenCV code that facilitated file preparation, image analysis, and organization of the results.

35th PLEA Conference. Planning Post Carbon Cities.
DOI: https://doi.org/10.17979/spudc.9788497497947

and designers make decisions on the design of the building façade in terms of its material and geometry.

6. LIMITATIONS AND FUTURE STUDIES

Although this proposed workflow has been proven to be extremely beneficial for the purpose of locating the building elements that cause glare, the execution of such a workflow requires knowledge of various disciplines, including architecture design and computer science. It is therefore clear that the methodology introduced in this paper could be difficult for the regular user, and further studies are required to devise an alternative workflow for non-programmers. A better approach for such users could be achieved using Grasshopper components, which use an easy-to-understand graphical user interface and hide complicated code from entry-level users.

6. REFERENCES

[1] Title: When Buildings Attack Their Neighbors: Strategies for Protecting Against " Death Rays " When Buildings Attack Their Neighbors: Strategies for Protecting Against " Death Rays " Façades, (2015). http://global.ctbuh.org/resources/papers/download/2100-when-buildings-attack-their-neighbors-strategies-for-protecting-against-death-rays.pdf.

[2] J.A. Jakubiec, C.F. Reinhart, Assessing Disability Glare Potential Due to Reflections from New Constructions : A Case Study Analysis and Recommendations for the Future, Transportation Research Record. (2014) 1–12. https://doi.org/10.3141/2449-13.

[3] R. Labib, J. Baltazar, Analysis and quantification of visual glare caused by photovoltaic panels installations in urban canyons, in: Advanced Building Skins, 2016.

[4] M. Jean-Jacques, D. Francioli, P. Rey, Observed variation of lighting conditions versus feelings of visual discomfort in VDT operators: Application of a new model, Lux Europa. (1993) 332–339.

[5] K.D. Garciai, W.W. Wierwille, Effect of Glare on Performance of a VDT Reading-Comprehension Task, Human Factors. 27 (1985) 163–173.

[6] A. Borisuit, F. Linhart, J.-L. Scartezzini, M. Munch, Effects of Realistic Office Daylighting and Electric Lighting Conditions on Visual Comfort, Alertness and Mood, Lighting Research and …. (2014) 1–18. https://doi.org/10.1177/1477153514531518.

[7] D.L. DiLaura, The Lighting Handbook: Reference & Application, Illuminating Engineering Society of North America, 2011.

[8] R.G. Hopkinson, Glare Discomfort and Pupil Diameter, Journal of the Optical Society of America. 46 (1956) 649–649. https://doi.org/10.1364/JOSA.46.000649.

[9] Y. Lin, S. Fotios, M. Wei, Y. Liu, W. Guo, Y. Sun, Eye Movement and Pupil Size Constriction Under Discomfort Glare, Investigative Ophthalmology and Visual Science. 56 (2015) 1649–1656. https://doi.org/10.1167/iovs.14-15963.

[10] C. Birnbaum, Museum Tower: “attack” on the Nasher Sculpture Center’s garden, building & art | The Cultural Landscape Foundation, (2012). https://tclf.org/blog/museum-tower-attack-nasher-sculpture-centers-garden-building-art (accessed December 10, 2017).

[11] S. Abdelwahab, M. Elhussainy, R. Labib, The Negative Impact of Solar Reflections Caused by Reflective Buildings’ Facades: Case Study of the Nasher Museum in Texas, IOP Conf. Ser.: Earth Environ. Sci. 297 (2019) 012048. https://doi.org/10.1088/1755-1315/297/1/012048.

[12] Skvark, opencv-python, PyPI. (2008). https://pypi.org/project/opencv-python/ (accessed September 7, 2018).

[13] Welcome to Python.org, Python.Org. (n.d.). https://www.python.org/ (accessed November 6, 2018).

[14] J. Suk, M. Schiler, Investigation of Evalglare Software, Daylight Glare Probability and High Dynamic Range Imaging for Daylight Glare Analysis, Lighting Research and Technology. 45 (2012) 450–463. https://doi.org/10.1177/1477153512458671.

[15] J. Wienold, Evalglare–A new RADIANCE-based tool to evaluate daylight glare in office spaces, in: 2004.

[16] A. Borisuit, J.-L. Scartezzini, A. Thanachareonkit, Visual discomfort and glare rating assessment of integrated daylighting and electric lighting systems using HDR imaging techniques, Architectural Science Review. 53 (2010) 359–373.

[17] R. Kittler, An historical review of methods and instrumentation for experimental daylight research by means of models and artificial skies: Proceedings of the 14th CIE session, Brussels: Commission Internationale de l’Eclairage. (1959).

[18] G.W. Larson, Rendering with Radiance: The Art and Science of Lighting Visualization, Morgan Kaufmann, 1998. http://books.google.com/books?id=DUpSAAAAMAAJ.

[19] Rhino for Windows, (1980). https://www.rhino3d.com/ (accessed August 28, 2018).

DOI: https://doi.org/10.17979/spudc.9788497497947

[20] J. Wienold, J. Christoffersen, Evaluation methods and development of a new glare prediction model for daylight environments with the use of CCD cameras, Energy and Buildings. 38 (2006) 743–757.
[21] R. Labib, JC. Baltazar, Automated Execution of Large-Scale Daylighting and Glare Simulations in a Cloud-Based Parallel Computing Environment, in: 16th IBPSA International Conference, Rome, Italy, 2019: p. 7.

DOI: https://doi.org/10.17979/spudc.9788497497947